Benchmark Calculations with Correlated Molecular Wave Functions. 11. Energetics of the Elementary Reactions F + H_2, O + H_2, and H′ + HCl

Kirk A. Peterson*

Department of Chemistry, Washington State University, and the Environmental Molecular Sciences Laboratory, Pacific Northwest National Laboratory, Richland, Washington 99352

Thom H. Dunning, Jr.†

Environmental Molecular Sciences Laboratory, Pacific Northwest National Laboratory, Richland, Washington 99352

Received: February 25, 1997; In Final Form: June 13, 1997⊗

An explicit treatment of electron correlation is required to predict accurate energetics, barrier heights, and saddle point geometries for chemical reactions. Several theoretical methods for treating electron correlation (multireference configuration interaction, perturbation theory, and coupled cluster methods) have been thoroughly evaluated for the F(^{2}P) + H_2($X^1\Sigma_g^+$) and O(^{3}P) + H_2($X^1\Sigma_g^+$) abstraction reactions as well as for the H′(^{2}S) + HCl($X^1\Sigma^+$) exchange reaction using correlation consistent basis sets. The basis set dependence of the reaction energy defects, barrier heights, and saddle point geometries have been determined for each theoretical method. Addition of diffuse functions to the basis set (aug-cc-pV*n*Z) was found to substantially increase the convergence rate. Calculations with the largest basis set (aug-cc-pV5Z) allowed an unambiguous comparison of the relative performance of each correlation method. For each reaction, the R-UCCSD(T) results closely parallel the most accurate MRCI results and are in good agreement with experiment. In contrast, unrestricted perturbation theory methods predict barriers that are too large by 2.7−4.4 kcal/mol (MP2), 3.5−4.2 kcal/mol (MP3), and 1.3−1.7 kcal/mol (MP4).

Introduction

In most modern *ab initio* electronic structure approaches to the calculation of molecular potential energy surfaces, the accuracy of the calculation is strongly dependent on two separate, yet intimately coupled, expansions. For the past three decades, most attention has been focused on developing more effective *n*-particle expansions, *i.e.*, the expansion of the electronic wave function in Slater determinants of molecular orbitals, because this expansion dictates the overall accuracy of the calculation. Beginning in the mid-1980s, however, it was recognized that the second expansion, the expansion of the molecular orbitals in a one-particle basis set, typically of Gaussian functions, can also dramatically affect the quality of the results. This led to the development of a number of basis sets for use in correlated calculations.[1−3] With the introduction of the correlation consistent gaussian basis sets developed by Dunning and co-workers,[4−9] it is now possible to efficiently approach the complete basis set (CBS) limit for any given correlation treatment.

The present study is one of a series of benchmark studies that take advantage of the systematic convergence of the correlation consistent basis sets to determine the *intrinsic accuracy* of a variety of correlation methods in use today. Previous studies have focused on the spectroscopic constants of a large number of diatomic and triatomic molecules,[10−15] the binding energies and structures of van der Waals and hydrogen-bonded species,[16,17] the geometry and energy of the saddle point for the H + H_2 reaction,[18] singlet−triplet splittings in C_2-like diatomics,[15] and the C−H bond dissociation energies in the CH_n and C_2H_n series.[19] In the present work, the accuracy and convergence of several correlation methods, including multireference configuration interaction (MRCI), coupled cluster [CCSD, CCSD(T)], and Møller−Pesset perturbation theory (MP2, MP3, MP4) are investigated for two elementary abstraction reactions (F + H_2 and O + H_2) and one exchange reaction (H′ + HCl).

Unlike the other benchmarking studies noted above, accurate experimental data for the three reactions considered here are only available for the reactants, products, and the reaction energy defect for the two abstraction reactions

$$\Delta E_{\mathrm{rxn}}(\mathrm{X}+\mathrm{H_2}) = D_{\mathrm{e}}(\mathrm{H_2}) - D_{\mathrm{e}}(\mathrm{HX})$$

where X = F, O. Direct experimental data is not available on the most interesting features of these reactions, namely, the geometries and energies of the saddle points. Nonetheless, the fact that the correlation consistent basis sets are able to accurately describe the barrier height and saddle point geometry for the H + H_2 reaction,[18] coupled with the convergence studies reported herein, give us confidence that the conclusions drawn about the performance of the various correlation methods are valid.

For all three reactions, previous calculations of barrier heights and transition state structures, as well as global potential energy surfaces, have been reported. Thus, the present work should prove valuable in the critical assessment of the quality of these (and future) potentials. In the case of the F + H_2 reaction, a global potential energy surface has been computed by Stark and Werner[20] using multireference configuration interation (MRCI) wave functions essentially identical to those used in the present work (see below) in conjunction with a basis set of nearly aug-cc-pV5Z quality. This surface has since been used in extensive dynamics calculations (e.g., ref 21) that have led to quantitative agreement with experimental results. Other previous calcula-

* Address correspondence to this author. E-mail: ka_peterson@pnl.gov.
† E-mail: th_dunning@pnl.gov.
⊗ Abstract published in *Advance ACS Abstracts,* August 1, 1997.

S1089-5639(97)00676-2 CCC: $14.00

tions have been reviewed in ref 20, Wright et al.,[22] and Schaefer.[23] There have been far less published work on the $O(^3P) + H_2$ reaction. The most accurate existing calculations are those of Walch,[24−26] where MRCI calculations with a large atomic natural orbital (ANO) basis set were carried out. A global surface obtained using similar methods to those in the present work is currently underway by Walch.[27] Numerous previous calculations have been carried out in order to characterize the exchange barrier for the H′ + HCl reaction, sparked in part by the disagreement with an early, and much too low, experimental estimate of the barrier height. The most accurate calculations to date are those of Schwenke *et al.*[28] and Allison *et al.*[29] who carried out predominately MRCI calculations with a large basis set and then corrected the results with the SEC (scaling of the external correlation energy) method.

Details of the Calculations

The basis sets used in the present work correspond to the standard correlation consistent basis sets, cc-pV*n*Z (*n* = D, T, Q, and 5), of Dunning and co-workers.[4,6] In addition, the augmented sets, aug-cc-pV*n*Z, derived [5,6] from the standard sets by addition of an extra set of diffuse functions for each angular momentum type present in the standard set were investigated. While the exponents of these extra functions were optimized at the CISD (singles and doubles configuration interaction) level of theory for the atomic anions and are required to accurately describe electron affinities, they have since been shown to systematically improve the description of a number of molecular properties such as the binding of weakly-interacting systems,[16,17,30−32] proton affinities,[33] and molecular dipole moments and polarizabilities.[7,17,34] The importance of these functions for describing the saddle points of the reactions considered in the present study is shown below.

For investigating the effects of correlating the first-level core electrons (1s for O and F, 2s2p for Cl), an augmented correlation consistent polarized weighted core−valence quadruple-zeta basis set,[35] denoted aug-cc-pwCVQZ, was utilized. These sets were derived from the standard aug-cc-pVQZ sets by adding additional spdf (and g for Cl) functions that were optimized explicitly for core−valence correlation in atomic calculations. These new sets differ from the previously published cc-pCV*n*Z sets[8] for the first-row atoms, in that the core−valence correlation energy (intershell) was strongly weighted over the core−core correlation energy (intrashell) in the optimization procedure. This new prescription has been shown to lead to faster convergence to the basis set limit for molecular core−valence correlation effects.[35]

By systematically increasing the quality of the one-particle basis set, regular convergence behavior toward a complete basis set (CBS) limit is often observed when correlation consistent basis sets are used. Frequently the basis set dependence is well described by simple exponential-like functions of the form

$$A_n = A_\infty + Be^{-Cn} \quad (1)$$

or

$$A_n = A_\infty + Be^{-(n-1)} + Ce^{-(n-1)^2} \quad (2)$$

where *n* is the cardinal number of the basis set (2, 3, 4, and 5 for DZ, TZ, QZ, and 5Z sets, respectively) and A_∞ corresponds to the estimated CBS limit as $n \rightarrow \infty$ for the molecular property A_n. In the present work, estimated CBS limits were obtained for properties such as the reaction energies and barrier heights by using eq 2. Very similar results were obtained with eq 1 when extrapolations of the separate total energies were used. Only by extrapolating to the CBS limit can the true or *intrinsic* accuracy of the correlation method be unambiguously determined. As demonstrated previously for the dissociation energy of the N_2 molecule,[14] incomplete basis sets can greatly obscure our understanding of the relative accuracy of different theoretical methods.

Electron correlation methods based on both Hartree−Fock (HF) and complete active space self-consistent field (CASSCF) wave functions have been used in the present work. The single configuration-based methods included single and doubles coupled cluster theory (CCSD) and CCSD with a perturbative estimate of triple excitations, CCSD(T).[36−39] In addition, second-, third-, and fourth-order Møller−Plesset perturbation theory,[40] MP2, MP3, and MP4, respectively, have also been used. Since all three of these reactions involve open-shell potential energy surfaces, the effects of using either a restricted open-shell Hartree−Fock (ROHF) or unrestricted HF (UHF) reference function has been investigated for the coupled cluster wave functions. The different variants of CCSD(T) that were used included the spin-restricted method of Werner and Knowles,[41] RCCSD(T); a method also based on ROHF orbitals but with small amounts of spin contamination allowed in the linear terms of the wave function, R-UCCSD(T);[41−43] and CCSD(T) based on a UHF reference, U-UCCSD(T).[37] For the perturbation theory results, UHF-based methods were used throughout (UMP2, UMP3, and UMP4). For the $O(^3P) + H_2$ reaction, where the lowest energy reaction path involves a $^3\Pi$ potential energy surface, the ROHF orbitals used in the RCCSD(T) and R-UCCSD(T) calculations were obtained from state-averaged ($\Pi_x + \Pi_y$) SCF calculations.

Two different active spaces were used in the CASSCF and subsequent internally contracted multireference configuration interaction[44,45] (denoted icMRCI or simply CAS+1+2) calculations. One of these (labeled "val") consisted of the standard full-valence active space, *i.e.*, all the molecular orbitals obtained from the atomic valence orbitals. For the present work, this corresponded to 9 (8 for $O + H_2$) electrons in 6 orbitals (4 of a_1, 1 of b_1, and 1 of b_2 symmetry in C_{2v}). The number of configuration state functions (CSFs) then totaled 28. The second active space (denoted "ext") was obtained by extending the full valence space by two additional orbitals of π_x and π_y symmetry (b_1 and b_2 in C_{2v}), for a 9 (8) in 8 CAS for a total of 616, 592, and 616 CSFs for $F + H_2$, $O + H_2$, and H′ + HCl, respectively. In the cases of $F + H_2$ and $O + H_2$, these additional orbitals were nominally F or O atomic $3p_\pi$ orbitals. In the case of H′ + HCl, they consisted of mostly Cl $3d_\pi$ character. A limited number of calculations for the H′ + HCl reaction were also carried out with an active space that included both the Cl $3d_\pi$ and $4p_\pi$ orbitals (denoted ext′, 6976 CSFs). In the case of F + H_2, the choice of active space was essentially identical to the previous work of Stark and Werner.[20]

In every case, measures were taken to minimize the mixing between the nominally core and 2s orbitals of F and O and the core and 3s orbitals of Cl. While the CASSCF wave function is invariant with respect to unitary transformations among these orbitals, the subsequent MRCI calculations are not since the core orbitals (1s for F and O and 1s2s2p for Cl) are not correlated. Poor resolution of frozen core orbitals can artificially raise MRCI energies and degrade the results. As in our previous work,[12,34] we have resolved the core orbitals by carring out a two-step CASSCF procedure. For instance, for $F + H_2$ and O + H_2, in the first step the first two orbitals of a_1 symmetry ($1-2\sigma$) were constrained to be doubly occupied in an otherwise valence-only active space; in this way they can be uniquely

defined as eigenfunctions of an effective Fock operator as described in ref 20. The first a_1 orbital from this calculation was then frozen and used in a second CASSCF with both active spaces described above. The procedure for the H′ + HCl reaction was carried out in an analogous manner to minimize the mixing between the core and 3s orbital of Cl. For the F + H_2 and H′ + HCl reactions, the extended (ext) CASSCF calculations constrained the nominally 2s (F) or 3s (Cl) orbitals to be doubly occupied even in the second CASSCF step outlined above. This facilitated obtaining a consistent set of active space orbitals for each set of geometries calculated (reactants, saddle point, and products). Subsequent internally contracted MRCI calculations were then carried out using CASSCF active spaces as the reference function (with only the core orbitals constrained to be doubly occupied). In each case, the frozen core approximation was used with either the full valence (28 CSFs) or extended active spaces (∼600 CSFs) described above. Furthermore, for the H′ + HCl reaction, CASSCF orbitals from the large $3d_\pi + 4p_\pi$ active space described above were also used in the ext-CAS+1+2 calculations due to symmetry breaking problems. The effects of higher excitations have been approximated by the addition of the multireference Davidson correction (CAS+1+2+Q).[46−48]

The geometries and energetics of the various reactants, products, and saddle points of the three reactions of the current study were calculated from polynomial fits of local potential energy surfaces. For the products and reactants, a total of seven points in C_{2v} symmetry were computed that approximately covered the range $-0.3\ a_0 \le r - r_e \le +0.5\ a_0$, where r_e is the diatomic (H_2, OH, HF, or HCl) equilibrium distance. In these cases, the distance from the diatomic to its atomic partner was typically 50−100 a_0. The diatomic potentials were then fit to sixth order polynomials in $(r - r_e)$. For the saddle points, a grid of 25 points was computed about the linear saddle points for each method and basis set. These points were then fit to quartic polynomials in the displacements $(r - r_e^{sadpt})$ of the two bond distances, *e.g.*, F−H and H−H for the F−H−H saddle point. Unlike the other two reactions, the true saddle point for the F + H_2 reaction has been shown to be nonlinear (cf. ref 20), hence small 3-D grids of points have also been calculated about the nonlinear transition state as a function of basis set using the R-UCCSD(T) method. The program Fit1d[49] was used for the diatomic potential energy functions (PEFs), while the program Surfit[50] was used in fitting the 2-D and 3-D triatomic PEFs.

All of the CASSCF, CAS+1+2, and ROHF-based calculations in this work were carried out with the molpro suite of *ab initio* programs.[51] The UHF-based calculations, however, were completed with the Aces2[52] and Gaussian94[53] programs. Due to program limitations it was not possible to carry out the UMP*n* calculations on the saddle points with the aug-cc-pV5Z basis set. Fortunately, the MRCI and R-UCCSD(T) calculations suggest that the aug-cc-pVQZ set provides nearly converged results. In all cases only the pure spherical harmonic components of the polarization functions were retained in the calculations.

Results

The calculated total energies, geometries, and energetics for the reactants, products, and saddle points of the F + H_2, O + H_2, and H′ + HCl reactions are summarized in Tables I−III, respectively, along with the available experimental data. It is important to note that the observed convergence of the energetics and saddle point geometries of these reactions is accompanied by a similar convergence in the energetics and geometries of reactants and products. That is, the observed convergence of the calculations is due to an increasingly more accurate description of the molecular systems, not to a fortuitous cancellation of errors.

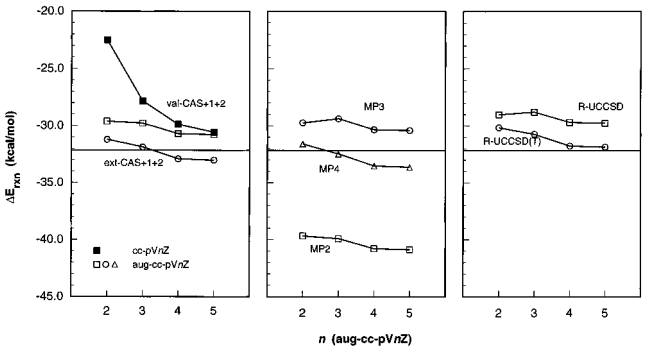

Figure 1. Calculated reaction energy defects, ΔE_{rxn}, for the F + H_2 abstraction reaction (in kcal/mol). The solid line is the experimental value for ΔE_{rxn}. Solid symbols denote the standard basis sets, open symbols the augmented basis sets.

F + H_2 → HF + H. Our calculated results for the reactants, products, and collinear saddle point for the F + H_2 reaction are listed in Table 1. Selected results for the reactants and products, which essentially correspond to the calculated spectroscopic constants of H_2 and HF, respectively, have appeared previously in our studies of H + H_2 (ref 18) and the HF dimer,[17] but are included here for completeness. For the F + H_2 asymptote, the differences among the MRCI methods merely reflect the lack of size consistency of the CI wave functions, since all of these are of full CI (FCI) quality for H_2 by itself. The CCSD results are identical to our previous FCI results for H_2.[18] In this case, the (T) triples correction only lowers the total energy of F atom. In general, the perturbation theory results for H_2 are in poorer agreement with experiment compared to CAS+1+2 or CCSD.

For the products HF + H, the CI methods are size consistent and in general perform as well as CCSD(T), which has been shown previously to yield excellent spectroscopic constants for the HF molecule.[17,54] In this case, use of the extended active space greatly improves the CAS+1+2 dissociation energy, increasing it by nearly 2.5 kcal/mol over the val-CAS+1+2 result with the aug-cc-pV5Z basis set. Including the Davidson correction, ext-CAS+1+2+Q yields a D_e with the aug-cc-pV5Z basis set that is only 0.4 kcal/mol smaller than experiment and nearly identical to that of CCSD(T). As noted in our previous work,[17] both MP2 and MP4 overshoot the experimental D_e of HF in the CBS limit. It should be noted that the experimental D_e for HF shown in Table 1 has had the spin−orbit coupling of the F atom[55] removed, *i.e.*, $D_e = D_e$ (expt) + $^1/_3[E(^2P_{1/2}) - E(^2P_{3/2})]$, which is appropriate for comparison to the present *ab initio* results, which do not include spin−orbit effects.

Also shown in Table 1 are the calculated reaction energy defects for the F + H_2 → HF + H reaction, together with an experimental value[56] that has also been adjusted for spin−orbit effects (−31.73 − 0.38 kcal/mol). The accuracy of the calculated defects is dependent on a balance between the errors in the calculated H_2 and HF bond dissociation energies. Nonetheless, with the standard correlation consistent basis sets, the reaction energy defect appears to converge smoothly with increasing basis set size; see Figure 1 and Table 1. The change in ΔE_{rxn} is far less pronounced for the augmented basis sets, and the convergence is not necessarily monotonic; see Figure 1. The aug-cc-pVQZ basis set appears to provide essentially converged results (±0.1 kcal/mol).

The val-CAS+1+2 method underestimates the magnitude of ΔE_{rxn} by 1.3 kcal/mol (aug-cc-pV5Z), while the ext-CAS+1+2

TABLE 1: Total Energies and Geometries of the Reactants, Products, and Saddle Point of the Collinear F(^{2}P) + H_2 Reaction, plus the Resulting Reaction Energy Defects and Barrier Heights Based on (A) Multireference and (B) Single Reference Wave Functions[a]

		F(^{2}P) + H_2			FH($^1\Sigma^+$) + H				F−H−H($^2\Sigma^+$)			
method	basis set	E_e	r_e(HH)	D_e	E_e	r_e(HF)	D_e	ΔE_{rxn}	E_e	r_e(HH)	r_e(HF)	ΔE_b
A. Multireference Wave Functions												
exptl[b]			0.7414	109.48		0.9168	141.58	−32.10				
val-CAS+1+2	cc-pVDZ	−100.685 896	0.7614	102.77	−100.721 748	0.9198	125.26	−22.50	−100.674 555	0.8083	1.3710	7.12
	cc-pVTZ	−100.782 028	0.7432	107.03	−100.826 358	0.9161	134.85	−27.82	−100.773 828	0.7780	1.4300	5.15
	cc-pVQZ	−100.811 495	0.7424	107.64	−100.859 112	0.9146	137.52	−29.88	−100.804 425	0.7743	1.4531	4.44
	cc-pV5Z	−100.821 587	0.7421	107.80	−100.870 294	0.9148	138.37	−30.56	−100.814 832	0.7732	1.4612	4.24
	aug-cc-pVDZ	−100.706 990	0.7620	103.22	−100.754 154	0.9228	132.81	−29.60	−100.701 028	0.7914	1.4860	3.74
	aug-cc-pVTZ	−100.788 546	0.7435	107.13	−100.835 993	0.9190	136.90	−29.77	−100.782 167	0.7741	1.4640	4.00
	aug-cc-pVQZ	−100.813 767	0.7425	107.66	−100.862 685	0.9157	138.36	−30.70	−100.807 510	0.7728	1.4666	3.93
	aug-cc-pV5Z	−100.822 500	0.7421	107.82	−100.871 538	0.9152	138.59	−30.77	−100.815 971	0.7728	1.4650	4.10
val-CAS+1+2+Q	cc-pVDZ	−100.691 517	0.7608	103.61	−100.727 710	0.9203	126.32	−22.71	−100.681 293	0.8038	1.3866	6.42
	cc-pVTZ	−100.791 447	0.7425	108.33	−100.836 331	0.9173	136.50	−28.17	−100.784 800	0.7719	1.4628	4.17
	cc-pVQZ	−100.822 211	0.7417	109.05	−100.870 554	0.9161	139.39	−30.34	−100.816 858	0.7677	1.4945	3.36
	cc-pV5Z	−100.832 716	0.7414	109.25	−100.882 241	0.9165	140.32	−31.08	−100.827 768	0.7664	1.5060	3.11
	aug-cc-pVDZ	−100.714 637	0.7616	104.28	−100.762 501	0.9245	134.32	−30.04	−100.710 235	0.7855	1.5294	2.76
	aug-cc-pVTZ	−100.798 757	0.7429	108.49	−100.846 965	0.9208	138.74	−30.25	−100.794 159	0.7674	1.5091	2.89
	aug-cc-pVQZ	−100.824 749	0.7419	109.09	−100.874 506	0.9175	140.31	−31.22	−100.820 308	0.7660	1.5136	2.79
	aug-cc-pV5Z	−100.833 709	0.7415	109.26	−100.883 599	0.9170	140.57	−31.31	−100.829 015	0.7660	1.5112	2.95
ext-CAS+1+2	aug-cc-pVDZ	−100.710 846	0.7620	103.45	−100.760 572	0.9243	134.66	−31.20	−100.707 214	0.7834	1.5578	2.28
	aug-cc-pVTZ	−100.793 549	0.7434	107.37	−100.844 322	0.9208	139.24	−31.86	−100.789 827	0.7643	1.5446	2.34
	aug-cc-pVQZ	−100.818 961	0.7424	107.90	−100.871 405	0.9175	140.81	−32.91	−100.815 431	0.7624	1.5547	2.22
	aug-cc-pV5Z	−100.827 766	0.7420	108.06	−100.880 386	0.9171	141.08	−33.02	−100.824 025	0.7625	1.5522	2.35
ext-CAS+1+2+Q	aug-cc-pVDZ	−100.715 680	0.7616	104.32	−100.763 879	0.9246	134.57	−30.25	−100.712 519	0.7821	1.5716	1.98
	aug-cc-pVTZ	−100.800 661	0.7429	108.54	−100.849 623	0.9212	139.26	−30.72	−100.797 540	0.7626	1.5621	1.96
	aug-cc-pVQZ	−100.826 753	0.7419	109.14	−100.877 361	0.9180	140.90	−31.76	−100.823 855	0.7604	1.5755	1.82
	aug-cc-pV5Z	−100.835 769	0.7415	109.32	−100.886 536	0.9176	141.17	−31.86	−100.832 672	0.7605	1.5727	1.94
B. Single Reference Wave Functions												
exptl[b]			0.7414	109.48		0.9168	141.58	−32.10				
UMP2	aug-cc-pVDZ	−100.691 916	0.7549	98.86	−100.755 138	0.9248	138.54	−39.67	−100.684 095	0.7883	1.4308	4.91
	aug-cc-pVTZ	−100.777 129	0.7375	103.78	−100.840 712	0.9218	143.68	−39.90	−100.769 409	0.7703	1.4190	4.84
	aug-cc-pVQZ	−100.804 716	0.7363	104.70	−100.869 709	0.9187	145.48	−40.78	−100.797 270	0.7691	1.4207	4.67
	aug-cc-pV5Z	−100.815 419	0.7359	105.03	−100.880 554	0.9184	145.90	−40.87				
UMP3	aug-cc-pVDZ	−100.708 393	0.7584	102.88	−100.755 781	0.9194	132.62	−29.74	−100.698 617	0.7995	1.3840	6.13
	aug-cc-pVTZ	−100.792 735	0.7399	107.26	−100.839 539	0.9156	136.63	−29.37	−100.782 904	0.7817	1.3679	6.17
	aug-cc-pVQZ	−100.818 951	0.7388	107.85	−100.867 290	0.9124	138.18	−30.33	−100.809 383	0.7805	1.3696	6.00
	aug-cc-pV5Z	−100.828 018	0.7384	108.02	−100.876 464	0.9120	138.42	−30.40				
UMP4	aug-cc-pVDZ	−100.714 062	0.7602	103.91	−100.764 393	0.9254	135.49	−31.58	−100.707 408	0.7931	1.4396	4.18
	aug-cc-pVTZ	−100.799 493	0.7416	108.17	−100.851 224	0.9227	140.63	−32.46	−100.793 319	0.7730	1.4371	3.87
	aug-cc-pVQZ	−100.825 846	0.7406	108.78	−100.879 246	0.9194	142.29	−33.51	−100.820 018	0.7715	1.4427	3.66
	aug-cc-pV5Z	−100.834 995	0.7402	108.96	−100.888 564	0.9191	142.58	−33.62				
R-UCCSD	aug-cc-pVDZ	−100.712 585	0.7617	104.31	−100.758 810	0.9222	133.32	−29.01	−100.707 952	0.7892	1.5031	2.91
	aug-cc-pVTZ	−100.795 986	0.7430	108.56	−100.841 866	0.9182	137.35	−28.79	−100.791 155	0.7717	1.4798	3.03
	aug-cc-pVQZ	−100.821 733	0.7420	109.17	−100.869 054	0.9149	138.86	−29.69	−100.817 158	0.7700	1.4875	2.87
	aug-cc-pV5Z	−100.830 623	0.7416	109.35	−100.878 042	0.9144	139.11	−29.76	−100.825 825	0.7700	1.4866	3.01
R-UCCSD(T)	aug-cc-pVDZ	−100.714 935	0.7617	104.31	−100.762 975	0.9241	134.46	−30.15	−100.711 560	0.7847	1.5477	2.12
	aug-cc-pVTZ	−100.800 407	0.7430	108.56	−100.849 398	0.9210	139.30	−30.74	−100.797 192	0.7657	1.5371	2.02
	aug-cc-pVQZ	−100.826 712	0.7420	109.17	−100.877 332	0.9177	140.93	−31.76	−100.823 802	0.7636	1.5498	1.83
	aug-cc-pV5Z	−100.835 850	0.7416	109.35	−100.886 627	0.9173	141.21	−31.86	−100.832 750	0.7635	1.5490	1.95

[a] Total energies are in hartrees; internuclear distances are in Å; and dissociation energies, reaction energy defects and barrier heights are in kcal/mol. [b] Reference 56.

method overestimates the magnitude of ΔE_{rxn} by 0.9 kcal/mol with the same basis set. The Davidson correction increases the magnitude of ΔE_{rxn} by 0.5 kcal/mol for the val-CAS+1+2 method and decreases the magnitude of ΔE_{rxn} by 1.2 kcal/mol for the ext-CAS+1+2 method. For the MRCI methods, the Davidson corrected results yield the most accurate values for ΔE_{rxn}; with the aug-cc-pV5Z basis set the ext-CAS+1+2+Q result is just 0.25 kcal/mol smaller in magnitude than experiment.

As discussed above, the CCSD(T) method yields excellent results for $D_e(H_2)$ and D_e(HF), hence it also predicts very accurate values for the reaction energy defect. With the aug-cc-pV5Z basis set, the R-UCCSD(T) method predicts a reaction energy defect of −31.86 kcal/mol, identical to that predicted by the ext-CAS+1+2+Q method and just 0.25 kcal/mol from the experimental value. Most of the remaining error is attributable to the neglect of core−valence correlation (see below). Addition of triple excitations to the R-UCCSD calculation is critical to achieving high accuracy, increasing the magnitude of ΔE_{rxn} by 2.1 kcal/mol.

For the MP*n* methods, both MP2 and MP4 overestimate ΔE_{rxn} in the CBS limit. With smaller basis sets, MP4 appears to yield an accurate value for the reaction energy defect, but this is due to comparable (and large!) errors in both $D_e(H_2)$ and D_e(HF). As the basis set is improved, $D_e(H_2)$ is underestimated and D_e(HF) overestimated, leading to a calculated reaction energy defect that is 1.5 kcal/mol below the experimental value (aug-cc-pV5Z). The MP3 method shows better behavior since it systematically underestimates the dissociation energies of both the reactants and products, although, near the basis set limit, ΔE_{rxn} is above experiment by 1.7 kcal/mol (aug-cc-pV5Z).

Calculated collinear saddle point properties for the F + H_2 reaction are also listed in Table 1 and plotted in Figures 2 (ΔE_b) and 3 [r_e(HH), r_e(HF)]. Both the cc-pV*n*Z and aug-cc-pV*n*Z

TABLE 2: Total Energies and Geometries of the Reactants, Products, and Saddle Point of the Collinear O(^{3}P) + H_2 Reaction, plus the Resulting Reaction Energy Defects and Barrier Heights, Based on (A) Multireference and (B) Single Reference Wave Functions[a]

		O(^{3}P) + H_2[b]			OH($^2\Pi$) + H				O−H−H($^3\Pi$)			
method	basis set	E_e	r_e(HH)	D_e	E_e	r_e(OH)	D_e	ΔE_{rxn}	E_e	r_e(HH)	r_e(OH)	ΔE_b
A. Multireference Wave Functions												
exptl[c]			0.7414	109.48		0.9697	106.6	2.88				
val-CAS+1+2	cc-pVDZ	−76.069 543	0.7614	102.85	−76.054 579	0.9798	93.46	9.39	−76.038 478	0.9493	1.1749	19.49
	cc-pVTZ	−76.137 960	0.7432	107.18	−76.128 860	0.9706	101.47	5.71	−76.110 886	0.9123	1.1931	16.99
	cc-pVQZ	−76.157 623	0.7424	107.81	−76.151 304	0.9688	103.85	3.97	−76.132 304	0.9017	1.2049	15.89
	cc-pV5Z	−76.164 084	0.7421	107.99	−76.158 715	0.9688	104.62	3.37	−76.139 346	0.8982	1.2100	15.52
	aug-cc-pVDZ	−76.084 289	0.7621	103.32	−76.076 979	0.9790	98.73	4.59	−76.059 598	0.9197	1.2136	15.49
	aug-cc-pVTZ	−76.142 279	0.7435	107.28	−76.135 559	0.9722	103.06	4.22	−76.117 467	0.9038	1.2066	15.57
	aug-cc-pVQZ	−76.159 055	0.7425	107.83	−76.153 701	0.9695	104.47	3.36	−76.134 686	0.8990	1.2096	15.29
	aug-cc-pV5Z	−76.164 645	0.7421	108.00	−76.159 559	0.9690	104.81	3.19	−76.140 195	0.8971	1.2119	15.34
val-CAS+1+2+Q	cc-pVDZ	−76.074 464	0.7608	103.62	−76.059 522	0.9802	94.25	9.38	−76.044 625	0.9475	1.1739	18.72
	cc-pVTZ	−76.146 137	0.7425	108.36	−76.137 153	0.9716	102.72	5.64	−76.121 067	0.9083	1.1949	15.73
	cc-pVQZ	−76.166 793	0.7418	109.08	−76.160 721	0.9700	105.27	3.81	−76.143 820	0.8963	1.2092	14.42
	cc-pV5Z	−76.173 567	0.7414	109.28	−76.168 526	0.9702	106.11	3.16	−76.151 345	0.8921	1.2156	13.94
	aug-cc-pVDZ	−76.091 143	0.7616	104.29	−76.084 028	0.9804	99.82	4.46	−76.068 626	0.9157	1.2170	14.13
	aug-cc-pVTZ	−76.151 199	0.7429	108.51	−76.144 765	0.9737	104.47	4.04	−76.128 892	0.8983	1.2114	14.00
	aug-cc-pVQZ	−76.168 471	0.7419	109.11	−76.163 464	0.9710	105.97	3.14	−76.146 686	0.8929	1.2154	13.67
	aug-cc-pV5Z	−76.174 198	0.7415	109.29	−76.169 474	0.9705	106.33	2.96	−76.152 341	0.8907	1.2180	13.72
ext-CAS+1+2	aug-cc-pVDZ	−76.086 935	0.7620	103.49	−76.081 164	0.9800	99.86	3.62	−76.064 370	0.9156	1.2187	14.16
	aug-cc-pVTZ	−76.145 573	0.7434	107.45	−76.140 965	0.9734	104.56	2.89	−76.123 390	0.8978	1.2140	13.92
	aug-cc-pVQZ	−76.162 444	0.7424	108.00	−76.159 336	0.9708	106.05	1.95	−76.140 832	0.8927	1.2178	13.56
	aug-cc-pV5Z	−76.168 068	0.7421	108.16	−76.165 266	0.9703	106.41	1.76	−76.146 405	0.8907	1.2204	13.59
ext-CAS+1+2+Q	aug-cc-pVDZ	−76.091 766	0.7616	104.32	−76.084 639	0.9802	99.85	4.47	−76.069 434	0.9196	1.2125	14.01
	aug-cc-pVTZ	−76.152 354	0.7429	108.55	−76.146 240	0.9737	104.71	3.84	−76.130 603	0.9017	1.2078	13.65
	aug-cc-pVQZ	−76.169 692	0.7419	109.15	−76.165 083	0.9711	106.26	2.89	−76.148 583	0.8963	1.2117	13.25
	aug-cc-pVQZ	−76.175 454	0.7415	109.33	−76.171 149	0.9706	106.63	2.70	−76.154 309	0.8941	1.2145	13.27
B. Single Reference Wave Functions												
exptl[c]						0.9697	106.6	2.88				
UMP2	aug-cc-pVDZ	−76.063 184			−76.064 906	0.9752	99.94	−1.08	−76.036 901	0.8714	1.2409	16.49
	aug-cc-pVTZ	−76.124 317			−76.126 158	0.9694	104.93	−1.16	−76.098 135	0.8588	1.2313	16.43
	aug-cc-pVQZ	−76.143 449			−76.146 583	0.9670	106.66	−1.97	−76.117 715	0.8559	1.2325	16.15
	aug-cc-pV5Z	−76.150 694			−76.154 137	0.9665	107.19	−2.16				
UMP3	aug-cc-pVDZ	−76.083 774			−76.077 203	0.9751	98.76	4.12	−76.055 425	0.8936	1.2153	17.79
	aug-cc-pVTZ	−76.144 334			−76.137 730	0.9684	103.11	4.14	−76.115 917	0.8802	1.2047	17.83
	aug-cc-pVQZ	−76.161 869			−76.156 703	0.9658	104.61	3.24	−76.133 907	0.8763	1.2071	17.55
	aug-cc-pV5Z	−76.167 671			−76.162 785	0.9653	104.95	3.07				
UMP4	aug-cc-pVDZ	−76.088 923			−76.082 565	0.9786	99.92	3.99	−76.063 324	0.8940	1.2233	16.06
	aug-cc-pVTZ	−76.149 931			−76.144 767	0.9727	104.93	3.24	−76.125 146	0.8759	1.2197	15.55
	aug-cc-pVQZ	−76.167 500			−76.163 888	0.9701	106.51	2.27	−76.143 324	0.8718	1.2230	15.17
	aug-cc-pV5Z	−76.173 371			−76.170 081	0.9697	106.90	2.06				
R-UCCSD	aug-cc-pVDZ	−76.088 591			−76.079 945	0.9777	98.89	5.43	−76.063 341	0.9306	1.1938	15.84
	aug-cc-pVTZ	−76.147 952			−76.139 412	0.9707	103.20	5.36	−76.122 494	0.9182	1.1834	15.98
	aug-cc-pVQZ	−76.165 047			−76.157 855	0.9679	104.66	4.51	−76.140 110	0.9132	1.1860	15.65
	aug-cc-pV5Z	−76.170 724			−76.163 792	0.9674	105.00	4.35	−76.145 734	0.9113	1.1880	15.68
R-UCCSD(T)	aug-cc-pVDZ	−76.090 467			−76.083 383	0.9796	99.87	4.45	−76.067 744	0.9167	1.2145	14.26
	aug-cc-pVTZ	−76.151 461			−76.145 368	0.9733	104.73	3.82	−76.129 391	0.8956	1.2136	13.85
	aug-cc-pVQZ	−76.169 001			−76.164 399	0.9707	106.28	2.89	−76.147 583	0.8907	1.2171	13.44
	aug-cc-pV5Z	−76.174 862			−76.170 567	0.9702	106.66	2.69	−76.153 416	0.8890	1.2193	13.46

[a] Total energies are in hartrees; internuclear distances are in Å; and dissociation energies, reaction energy defects, and barrier heights are in kcal/mol. [b] Spectroscopic constants of O+ H_2 are identical to those of Table 1B for F + H_2. [c] Reference 56.

basis set series are shown for the val-CAS+1+2 wave functions. As can be seen, the augmenting functions dramatically decrease the barrier heights obtained with the smaller basis sets, thereby greatly speeding up the convergence of this quantity. This has been previously attributed to the strong F^- character of the saddle point.[57] Even so, the standard basis sets still show well behaved, albeit slow, convergence toward the same apparent CBS limit as the augmented basis sets. At the quintuple zeta level the barriers predicted by these two basis set sequences differ by just 0.14 kcal/mol. Although the barrier heights calculated using the augmented sets result in significantly lower barriers for the smaller basis sets, the convergence characteristics are not as systematic. As shown by Stark and Werner,[20] this is primarily due to BSSE (basis set superposition error) effects, especially from the diffuse functions on hydrogen.

Addition of the multireference Davidson correction has a substantial effect on the computed CAS+1+2 barrier heights, *e.g.*, with the aug-cc-pV5Z basis set the +Q results differ from the CAS+1+2 values by 1.15 and 0.41 kcal/mol for the valence and extended active spaces, respectively. Based on the FCI study of Knowles *et al.*,[58] a CAS+1+2+Q calculation with an extended active space like the one used in this work is expected to give the most accurate results for the energetics of the F + H_2 reaction. As shown in Table 1, use of the larger reference space wave function lowers the barrier by over 1 kcal/mol for both CAS+1+2 and CAS+1+2+Q. Thus, our best directly calculated barrier height is presumably represented by the ext-CAS+1+2+Q/aug-cc-pV5Z value of 1.94 kcal/mol. This is larger by about 0.17 kcal/mol than that of Stark and Werner,[20] who used identical basis sets and correlation methods, but with slightly different molecular orbitals and reference functions. Using four-point fits with eq 2, the ext-CAS+1+2/CBS barrier height is estimated to be 2.29 kcal/mol, while the ext-CAS+1+2+Q value is 1.88 kcal/mol. The uncertainty in the

TABLE 3: Total Energies and Geometries of the Reactants, Products, and Saddle Point of the Collinear H′(^{2}S) + ClH($^1\Sigma^+$) Reaction, plus the Resulting Reaction Energy Barrier Heights Based on (A) Multireference and (B) Single Reference Wave Functions[a]

		H′(^{2}S) + HCl($^1\Sigma^+$)			H′−Cl−H($^2\Sigma_g^+$)		
method	basis set	E_e	r_e(HCl)	D_e	E_e	r_e(HCl)	ΔE_b
		A. Multireference Wave Functions					
exptl[b]			1.2746	107.32			
val-CAS+1+2	cc-pVDZ	−460.747 802	1.2905	97.58	−460.709 673	1.5138	23.93
	cc-pVTZ	−460.822 364	1.2769	102.83	−460.787 952	1.4927	21.59
	cc-pVQZ	−460.844 635	1.2759	104.76	−460.811 688	1.4871	20.67
	cc-pV5Z	−460.851 758	1.2746	105.54	−460.819 583	1.4831	20.19
	aug-cc-pVDZ	−460.762 778	1.2921	99.89	−460.727 662	1.5107	22.04
	aug-cc-pVTZ	−460.827 160	1.2780	103.67	−460.794 033	1.4911	20.79
	aug-cc-pVQZ	−460.846 295	1.2764	105.07	−460.813 843	1.4870	20.36
	aug-cc-pV5Z	−460.852 689	1.2749	105.70	−460.820 725	1.4831	20.06
val-CAS+1+2+Q	cc-pVDZ	−460.755 338	1.2903	98.30	−460.718 601	1.5103	23.05
	cc-pVTZ	−460.836 513	1.2772	104.00	−460.804 298	1.4897	20.21
	cc-pVQZ	−460.860 764	1.2765	106.13	−460.830 263	1.4843	19.14
	cc-pV5Z	−460.868 460	1.2754	106.95	−460.838 809	1.4805	18.61
	aug-cc-pVDZ	−460.772 442	1.2927	100.85	−460.739 184	1.5085	20.87
	aug-cc-pVTZ	−460.842 034	1.2786	104.91	−460.811 286	1.4886	19.29
	aug-cc-pVQZ	−460.862 635	1.2772	106.47	−460.832 696	1.4845	18.79
	aug-cc-pV5Z	−460.869 492	1.2757	107.13	−460.840 085	1.4806	18.45
ext-CAS+1+2	aug-cc-pVDZ	−460.766 777	1.2913	100.39	−460.731 929	1.5094	21.87
	aug-cc-pVTZ	−460.833 822	1.2768	104.32	−460.800 774	1.4898	20.74
	aug-cc-pVQZ	−460.853 522	1.2751	105.79	−460.821 071	1.4858	20.36
	aug-cc-pV5Z	−460.860 146	1.2736	106.45	−460.828 150	1.4818	20.08
ext-CAS+1+2+Q	aug-cc-pVDZ	−460.772 638	1.2928	100.75	−460.739 718	1.5082	20.66
	aug-cc-pVTZ	−460.843 795	1.2789	104.77	−460.813 382	1.4887	19.08
	aug-cc-pVQZ	−460.864 722	1.2774	106.33	−460.835 093	1.4847	18.59
	aug-cc-pV5Z	−460.871 703	1.2760	107.00	−460.842 589	1.4809	18.27
ext′-CAS+1+2	aug-cc-pVQZ	−460.856 354	1.2764	106.07	−460.825 295	1.4864	19.49
ext′-CAS+1+2+Q	aug-cc-pVQZ	−460.865 885	1.2778	106.45	−460.836 588	1.4850	18.38
		B. Single Reference Wave Functions					
exptl[b]			1.2746	107.32			
CCSD/R-UCCSD	aug-cc-pVDZ	−460.767 655	1.2906	99.89	−460.732 785	1.5040	21.88
	aug-cc-pVTZ	−460.834 546	1.2767	103.57	−460.802 169	1.4838	20.32
	aug-cc-pVQZ	−460.854 336	1.2753	104.95	−460.822 812	1.4798	19.78
	aug-cc-pV5Z	−460.860 988	1.2739	105.59	−460.830 021	1.4759	19.43
CCSD(T)/R-UCCSD(T)	aug-cc-pVDZ	−460.771 636	1.2922	100.89	−460.738 640	1.5067	20.71
	aug-cc-pVTZ	−460.843 062	1.2789	104.94	−460.813 053	1.4872	18.83
	aug-cc-pVQZ	−460.864 115	1.2776	106.37	−460.835 088	1.4836	18.21
	aug-cc-pV5Z	−460.871 288	1.2762	107.04	−460.842 857	1.4797	17.84
MP2/UMP2	aug-cc-pVDZ	−460.751 157	1.2880	100.61	−460.710 663	1.4873	25.41
	aug-cc-pVTZ	−460.814 951	1.2747	105.41	−460.777 876	1.4664	23.27
	aug-cc-pVQZ	−460.836 047	1.2734	107.00	−460.800 032	1.4623	22.60
	aug-cc-pV5Z	−460.844 776	1.2721	108.60			
MP3/UMP3	aug-cc-pVDZ	−460.767 416	1.2891	100.53	−460.728 701	1.4885	24.29
	aug-cc-pVTZ	−460.835 286	1.2754	104.62	−460.799 720	1.4689	22.32
	aug-cc-pVQZ	−460.855 665	1.2744	106.00	−460.821 066	1.4653	21.71
	aug-cc-pV5Z	−460.862 528	1.2730	107.39			
MP4/UMP4	aug-cc-pVDZ	−460.771 222	1.2913	101.06	−460.735 173	1.4926	22.62
	aug-cc-pVTZ	−460.842 744	1.2783	105.37	−460.809 954	1.4741	20.58
	aug-cc-pVQZ	−460.863 860	1.2773	106.85	−460.832 125	1.4708	19.91
	aug-cc-pV5Z	−460.870 957	1.2759	108.30			

[a] Total energies are in hartrees; internuclear distances are in Å; and dissociation energies and reaction energy barrier heights are in kcal/mol. [b] Reference 56.

extrapolation is estimated to be less than ±0.1 kcal/mol, and in each case the estimated CBS limit is nearly midway between the aug-cc-pVQZ and aug-cc-pV5Z values.

Also shown in Table 1 and Figures 2 and 3 are the results for F + H_2 using the R-UCCSD(T) and UMP*n* methods. In general, the R-UCCSD(T) results for the collinear saddle point are nearly identical to the ext-CAS+1+2+Q results, especially with the larger basis sets. For the UMP*n* methods, the calculated barrier heights are much larger than those obtained with either ext-CAS+1+2 or R-UCCSD(T). They also exhibit an oscillation whereby the MP2 value is too high, the MP3 result is higher again by nearly 1.5 kcal/mol, and the MP4 barrier height is lower than MP2 but still higher than the R-UCCSD(T) result by a factor of 2: 3.66 vs 1.83 kcal/mol with the aug-cc-pVQZ basis set. As shown previously by Schlegel and Sosa,[59] spin

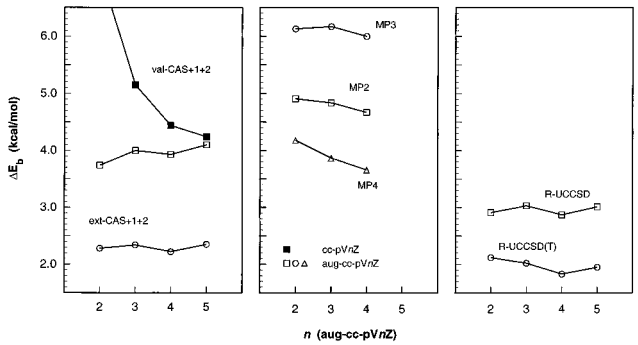

Figure 2. Calculated barrier heights, ΔE_b, for the F + H_2 abstraction reaction (in kcal/mol). Solid symbols denote the standard basis sets, open symbols the augmented basis sets.

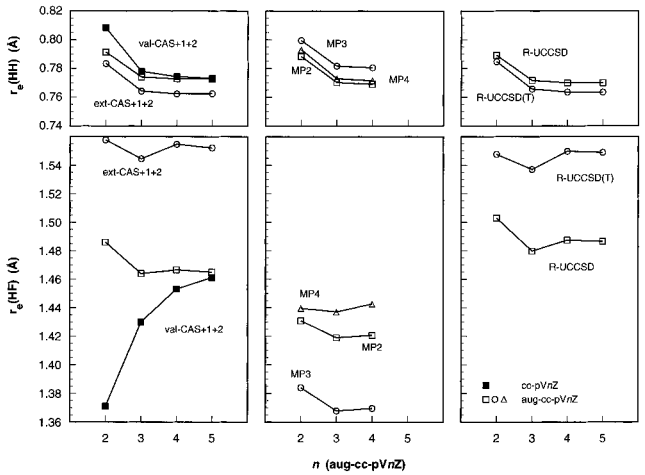

Figure 3. Calculated saddle point geometries, r_e(HH) and r_e(HF), for the F + H_2 abstraction reaction (in Å). Solid symbols denote the standard basis sets, open symbols the augmented basis sets.

projection decreases the UMP4 barrier for this reaction by ~1.3 kcal/mol, which would leave the MP4 value about 0.5 kcal/mol above the R-UCCSD(T) result.

Also shown in Table 1 are the computed geometries for the collinear saddle point with each method and basis set. As is well-known for this reaction, the saddle point occurs very early; the H−H distance at the saddle point, r_e(HH), is only about 3% longer than in H_2, while the H−F distance is nearly 70% longer than the equilibrium bond length in HF. In general, r_e(HH) at the saddle point converges monotonically as the basis set increases in size and does not show a large dependence on the correlation method used; see Figure 3. A far larger variation is observed for r_e(HF), *e.g.*, the ext-CAS+1+2 value is longer than the val-CAS+1+2 result by more than 0.085 Å. The saddle point geometry (aug-cc-pV5Z) predicted by the R-UCCSD(T) method agrees reasonably well with that obtained from ext-CAS+1+2+Q [r_e(HF) is 1.549 Å vs 1.573 Å], while the UMP4 value for r_e(HF) is much too short (1.443 Å).

Since the true saddle point for the F + H_2 abstraction reaction has been previously shown to be nonlinear, albeit with a very shallow bending potential, the nonlinear saddle point has also been characterized in this work with the R-UCCSD(T) method. The results are summarized in Table 4. With the aug-cc-pV5Z basis set, the R-UCCSD(T) method predicts a barrier height of 1.54 kcal/mol at a geometry of r_e(HH) = 0.773 Å, r_e(HF) = 1.526 Å, and θ_e(HHF) = 117.6°. These differ from their collinear values by −0.41 kcal/mol, +0.010 Å, −0.023 Å, and −62.4°, for the barrier height and geometry, respectively. Extrapolation to the estimated CBS limit yields a bent transition state barrier height of 1.45 kcal/mol, which differs from the collinear CBS limit by −0.42 kcal/mol. The large angular approach channel associated with the nonlinear saddle point will substantially increase the rate of the F + H_2 reaction. Earlier attempts to define an effective barrier height for the F + H_2 reaction by matching to experimental data used model surfaces that did not show this feature and it is now well recognized that the barrier heights so derived are incorrect. The most recent icMRCI+Q calculations of Stark and Werner[20] (see also ref 21) indicate that the R-UCCSD(T) results given above provide a quantitatively correct description of the F + H_2 reaction.

In general, the saddle point properties of the F + H_2 reaction show significant dependence on the detailed form of the open-shell CCSD(T) wave function. The different variants of open-shell CCSD(T) are compared in Table 5 for the collinear "saddle point." The RCCSD(T) method yields a value for the barrier height that is higher than those obtained with the R-UCCSD(T), U-UCCSD(T), and ext-CAS+1+2+Q methods. In addition, the calculated r_e(HF) at the saddle point for the RCCSD(T) method is almost 0.04 Å shorter than that of the R-UCCSD(T), U-UCCSD(T), and ext-CAS+1+2 methods. Use of UHF orbitals has a negligible effect, as indicated by the difference between the R-UCCSD(T) and U-UCCSD(T) results. Hence, spin relaxation in the CCSD equations is very effective. Fitting the local potential energy functions for the saddle point indicated a further problem with the RCCSD(T) method—the R-UCCSD(T) and U-UCCSD(T) total energies yielded significantly smoother fits than did the RCCSD(T) energies with root mean square (rms) deviations comparable to those of the CAS+1+2 potential energy functions.

The effects of core correlation have also been investigated with the R-UCCSD(T) method and the aug-cc-pwCVQZ basis set as described above; the results are summarized in Table 6. Both the reactant, product, and saddle point geometries were frozen at the valence-only aug-cc-pVQZ values, but this is not expected to significantly affect the computed core contributions to the reaction energetics. Both valence-only and all-electron calculations were carried out with the core−valence basis set to obtain the core contributions to the barrier height and reaction energy defects. As expected, correlation of the 1s-like core electrons of F has almost no effect on the computed barrier height, just +0.01 kcal/mol. However, the effect on the reaction energy defect, −0.17 kcal/mol, which corresponds to a core contribution to the dissociation energy of HF (+0.17 kcal/mol), is nonnegligible. When added to the R-UCCSD(T)/aug-cc-pV5Z value for ΔE_{rxn} (−31.86 kcal/mol), the resulting reaction energy defect (−32.03 kcal/mol) is only 0.08 kcal/mol above the experimental value.

Before leaving this section, let us compare the present results with selected results from prior calculations. The extrapolated CBS collinear barrier height of 1.88 kcal/mol compares very well with the limit estimated by Stark and Werner[20] of 1.83 ± 0.05 kcal/mol. The MRCI calculations of Wright et al.,[60] where the basis set included a set of bond functions, resulted in a collinear barrier height of 1.8 kcal/mol, but compared to the present calculations the location of their barrier is later along the reaction coordinate by about 6%. The bent saddle point was calculated by R-UCCSD(T)/aug-cc-pV5Z to lie 0.41 kcal/mol below the collinear saddle point for a resulting barrier height of 1.54 kcal/mol (extrapolation to the CBS limit is expected to decrease the barrier to about 1.45 kcal/mol). This result is in quantitative agreement with the previous MRCI calculations of Stark and Werner[20] and the R-UCCSD(T) work of Scuseria.[61] Other recent CCSD(T) calculations on the nonlinear barrier height of the F + H_2 reaction includes those of Kraka *et al.*[62] who used the standard cc-pVQZ basis set. Their computed barrier height of 2.17 kcal/mol is higher than the present results due to the lack of diffuse functions in the basis set. The lack of a sufficiently diffuse basis set also yielded a later saddle point (shorter F−H and longer H−H distances) in their calculations. Our MP4 calculations of the collinear reaction can be compared to the earlier work of Frisch *et al.*,[63] where ΔE_b was calculated to be 3.68 kcal/mol with basis sets of [7s5p3d2f] on F and [4s3p2d] on H. A more detailed comparison of our current results with the plethora of previous calculations is outside the scope of this work; the reader is referred to the recent papers of Stark and Werner[20] and Wright *et al.*[60] for more detailed discussions of previous calculations.

O + H_2 → OH + H. Results for the reactants, products, and saddle point for the O(^{3}P) + H_2 reaction are shown in Table 2. The MRCI-based spectroscopic constants for the reactants, O + H_2, are nearly identical to those shown previously for F +

TABLE 4: Total Energies and Geometries of the Nonlinear Saddle Point for the F(^{2}P) + H_2 Reaction Calculated with R-UCCSD(T)[a]

basis set	E_e	r_e(HH)	r_e(HF)	θ(HHF)	ΔE_b	E_b(bent) − E_b(collinear)
aug-cc-pVDZ	−100.711 917	0.7914	1.5251	125.53	1.89	−0.23
aug-cc-pVTZ	−100.797 582	0.7735	1.5182	124.58	1.77	−0.25
aug-cc-pVQZ	−100.824 327	0.7726	1.5281	119.14	1.50	−0.33
aug-cc-pV5Z	−100.833 396	0.7731	1.5258	117.59	1.54	−0.41

[a] Total energies are in hartrees; internuclear distances are in Å; angles are in degrees; and barrier heights are in kcal/mol.

TABLE 5: Comparison of CCSD(T) Methods with CAS+1+2+Q for Total Energies and Geometries of the Reactants, Products, and Saddle Point of the Collinear F + H_2, O + H_2, and H′ + ClH Reactions, plus the Resulting Reaction Energy Defects and Barrier Heights

	(F,O) + H_2			(F,O)H + H/H′+HCl				F−H−H/H′−Cl−H			
method	E_e	r_e(HH)	D_e	E_e	r_e(HX)	D_e	ΔE_{rxn}	E_e	r_e(HH)	r_e(HX)	ΔE_b
F + H_2											
exptl[b]		0.7414	109.48		0.9168	141.58	−32.10				
RCCSD(T)	−100.826 532	0.7420	109.17	−100.877 332	0.9177	141.05	−31.88	−100.823 035	0.7668	1.5109	2.19
R-UCCSD(T)	−100.826 712	0.7420	109.17	−100.877 332	0.9177	140.93	−31.76	−100.823 802	0.7636	1.5498	1.83
U-UCCSD(T)	−100.826 775	0.7420	109.17	−100.877 332	0.9177	140.89	−31.73	−100.823 868	0.7634	1.5521	1.82
ext-CAS+1+2+Q	−100.826 753	0.7419	109.14	−100.877 361	0.9180	140.90	−31.76	−100.823 855	0.7604	1.5755	1.82
O + H_2											
exptl[b]		0.7414	109.48		0.9697	106.6	2.88				
RCCSD(T)	−76.168 713	0.7420	109.17	−76.164 176	0.9705	106.32	2.85	−76.146 352	0.8799	1.2249	14.03
R-UCCSD(T)	−76.169 001	0.7420	109.17	−76.164 399	0.9707	106.28	2.89	−76.147 583	0.8907	1.2171	13.44
U-UCCSD(T)	−76.169 135	0.7420	109.17	−76.164 443	0.9706	106.22	2.94	−76.147 722	0.8944	1.2129	13.44
ext-CAS+1+2+Q	−76.169 692	0.7419	109.15	−76.165 083	0.9711	106.26	2.89	−76.148 583	0.8963	1.2117	13.25
H + ClH											
exptl[b]					1.2746	107.32	0.0				
RCCSD(T)				−460.864 115	1.2776	106.55	0.0	−460.834 401		1.4818	18.65
R-UCCSD(T)				−460.864 115	1.2776	106.37	0.0	−460.835 088		1.4836	18.21
U-UCCSD(T)				−460.864 115	1.2776	106.35	0.0	−460.835 001		1.4835	18.27
ext′-CAS+1+2+Q				−460.865 885	1.2778	106.45	0.0	−460.836 588		1.4850	18.38

[a] Total energies are in hartrees; internuclear distances are in Å; and dissociation energies, reaction energy defects, and barrier heights are in kcal/mol. All results use the aug-cc-pVQZ basis set. [b] Reference 56.

TABLE 6: Effect of Including Core and Core−Valence Correlation Effects on the Energetics of the F + H_2, O + H_2, and H′ + ClH Reactions Evaluated with the R-UCCSD(T) Method[a]

		(F,O) + H_2			(F,O)H + H/H+HCl				F−H−H/H−Cl−H			
method	basis set	E_e	r_e(HH)	D_e	E_e	r_e(HX)	D_e	ΔE_{rxn}	E_e	r_e(HH)	r_e(HX)	ΔE_b
F + H_2												
exptl			0.7414	109.48		0.9168	141.58	−32.10				
valence electron	aug-cc-pVQZ	−100.826 712	0.7420	109.17	−100.877 332	0.9177	140.93	−29.69	−100.823 802	0.7636	1.5498	1.83
valence electron	aug-cc-pwCVQZ	−100.829 798	(0.7420)	109.17	−100.880 169	(0.9177)	140.78	−31.61	−100.826 731	(0.7636)	(1.5498)	1.92
all electron	aug-cc-pwCVQZ	−100.891 548	(0.7420)	109.17	−100.942 199	(0.9177)	140.95	−31.78	−100.888 478	(0.7636)	(1.5498)	1.93
O + H_2												
extpl			0.7414	109.48			106.6	2.88				
valence electron	aug-cc-pVQZ	−76.169 001	0.7420	109.17	−76.164 399	0.9707	106.28	2.89	−76.147 583	0.8907	1.2171	13.44
valence electron	aug-cc-pwCVQZ	−76.170 999	(0.7420)	109.17	−76.166 319	(0.9707)	106.23	2.94	−76.149 429	(0.8907)	(1.2171)	13.54
all electron	aug-cc-pwCVQZ	−76.229 751	(0.7420)	109.17	−76.225 296	(0.9707)	106.37	2.80	−76.208 219	(0.8907)	(1.2171)	13.51
H + ClH												
exptl						1.2746	107.32					
valence electron	aug-cc-pVQZ				−460.864 115	1.2776	106.37		−460.835 088		1.4836	18.21
valence electron	aug-cc-pwCVQZ				−460.867 831	(1.2776)	106.74		−460.839 294		(1.4836)	17.91
all electron[d]	aug-cc-pwCVQZ				−461.191 843	(1.2776)	106.93		−461.163 233		(1.4836)	17.95

[a] Total energies are in hartrees; internuclear distances are in Å; and dissociation energies, reaction energy defects, and barrier heights are in kcal/mol. Values in parentheses are frozen at their valence-only aug-cc-pVQZ values. [b] Includes only the 2s and 2p core orbitals in addition to the 3s and 3p valence orbitals.

H_2 (Table 1). Since the SCF-based methods are size consistent, the spectroscopic constants for H_2 are identical to those of Table 1. The calculated val-CAS+1+2 bond lengths and dissociation energies shown in Table 2 for the OH product are identical to our previous work. As for the HF molecule, the addition of the multireference Davidson correction contributes about 1.5 kcal/mol to the calculated D_e for OH and leads to much better agreement with experiment. Expanding the reference space significantly decreases the impact of the +Q correction on the dissociation energy; the difference between the ext-CAS+1+2 and ext-CAS+1+2+Q values of D_e with the aug-cc-pV5Z basis set is just 0.22 kcal/mol. With the aug-cc-pV5Z basis set, the ext-CAS+1+2+Q bond length is too long by just 0.001 Å. The dissociation energy (D_e) at this level of theory, 106.63 kcal/

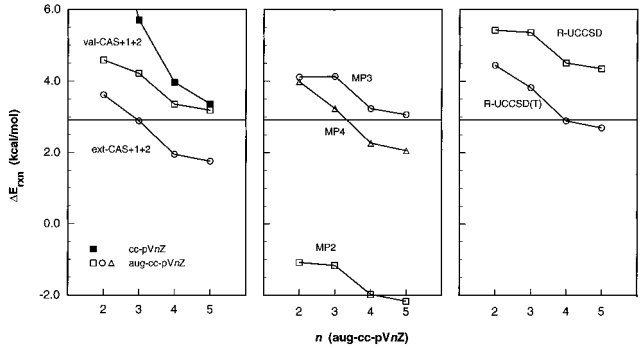

Figure 4. Calculated reaction energy defects, ΔE_{rxn}, for the O + H_2 abstraction reaction (in kcal/mol). The solid line is the experimental value for ΔE_{rxn}. Solid symbols denote the standard basis sets, open symbols the augmented basis sets.

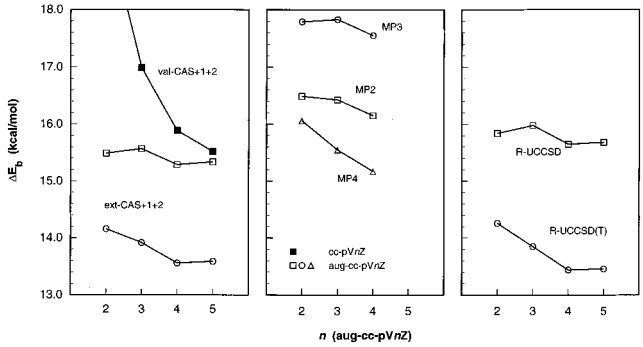

Figure 5. Calculated barrier heights, ΔE_b, for the O + H_2 abstraction reaction (in kcal/mol). Solid symbols denote the standard basis sets, open symbols the augmented basis sets.

mol, is essentially identical to the experimental value[56] (corrected for both molecular and atomic spin−orbit coupling). However, further basis set extensions are estimated to further increase D_e at this level of theory by another 0.2−0.3 kcal/mol.

Of the SCF-based methods shown in Table 2b, the R-UCCSD(T) results agree most closely with the ext-CAS+1+2+Q values for D_e and r_e. In contrast to the previous results for HF, the MP2 and MP4 methods yield r_e and D_e values in good agreement with experiment for OH (MP3 as usual underestimates both D_e and r_e).

The difference between the calculated bond dissociation energies of H_2 and OH yields the reaction energy defect for the (endothermic) O + H_2 reaction. As shown in Table 2 and Figure 4, due to the systematic convergence of the individual D_e's toward their respective CBS limits, the calculated ΔE_{rxn}'s also exhibit well-behaved convergence with respect to extension of the basis set. For the MRCI results shown in Table 2a, both val-CAS+1+2 and val-CAS+1+2+Q yield reaction energies that are only slightly larger than the experimental value of 2.88 kcal/mol. In both cases this is the result of a cancellation of errors due to a systematic underestimation of both bond dissociation energies. The cancellation is particularly large for val-CAS+1+2, where the two D_e's are each too small by approximately $1^1/_2$ kcal/mol (aug-cc-pV5Z). While the +Q correction improves both D_e's by nearly 1.5 kcal/mol, the resulting ΔE_{rxn} differs from the CAS+1+2 value by just 0.22 kcal/mol. With the aug-cc-pV5Z basis set, the calculated val-CAS+1+2+Q energy defect is in nearly perfect agreement with experiment, since both $D_e(H_2)$ and D_e(OH) are underestimated by about 0.2−0.3 kcal/mol. Extension of the active space as indicated by the ext-CAS+1+2 results leads to a much larger increase in D_e(OH) compared to $D_e(H_2)$, and hence the calculated ΔE_{rxn} becomes somewhat smaller than experiment.

The energy defect obtained with the R-UCCSD(T) method (2.69 kcal/mol) is nearly identical to that obtained with the ext-CAS+1+2+Q method (2.70 kcal/mol), and is just 0.19 kcal/mol smaller than the experimental value (2.88 kcal/mol). The value of ΔE_{rxn} obtained with the aug-cc-pVQZ basis set (2.89 kcal/mol) is essentially identical to that obtained from experiment, but the agreement is clearly fortuitous—the basis set expansion has not yet converged. Inclusion of triple excitations in the coupled cluster calculations decreases ΔE_{rxn} by 1.7 kcal/mol, slightly less than in F + H_2 (2.1 kcal/mol).

Due to the poor performance of the MP2 method for H_2, this method actually predicts an negative reaction energy defect for O + H_2, with the magnitude increasing with basis set size to −2.16 kcal/mol with the aug-cc-pV5Z set. The MP3 method with the aug-cc-pV5Z basis set yields a value for ΔE_{rxn} in good agreement with the experimental value, 3.07 vs 2.88 kcal/mol. The energy defect calculated by MP4, on the other hand, is too small by 0.6 kcal/mol due to the underestimation of $D_e(H_2)$ and overestimation of D_e(OH) as the CBS limit is approached.

Since the O + H_2 reaction is nearly thermoneutral, the saddle point is expected to be centrally located and the barrier to reaction large. This is borne out by the present calculations of the collinear saddle point, where the calculated r_e(HH) is ∼21% longer than the equilibrium distance in H_2, and r_e(OH) is ∼25% longer than that of the OH radical. The calculated barrier heights in Table 2 are also far larger than those in Table 1. The val-CAS+1+2 calculations predict a ΔE_b of 15.34 kcal/mol (with the aug-cc-pV5Z set). The effect of higher excitations, as estimated by the +Q correction, is somewhat more than 1.5 kcal/mol, bringing the barrier height down to 13.72 kcal/mol (aug-cc-pV5Z). Analogous to the F + H_2 reaction, O(2p → 2p′) excitations in the reference wave function strongly affect the calculated barrier height: the ext-CAS+1+2 wave function yields a ΔE_b of 13.59 kcal/mol (aug-cc-pV5Z), which is 1.93 kcal/mol lower than the val-CAS+1+2 result. The ext-CAS+1+2 barrier height is lower by another 0.32 kcal/mol with the +Q correction, yielding our best calculated value for ΔE_b of 13.27 kcal/mol.

For the HF-based methods shown in Table 2b, the UMP*n* results have an oscillatory behavior similar to that observed for F + H_2; see Figure 5. With the aug-cc-pVQZ basis set, the UMP4 barrier height, 15.17 kcal/mol, is nearly 2 kcal/mol higher than that of ext-CAS+1+2+Q. The barrier heights obtained with the UMP2 and UMP3 methods are higher still, 16.15 and 17.55 kcal/mol (aug-cc-pVQZ basis), respectively. The R-UCCSD(T) value for ΔE_b, on the other hand, is only 0.2 kcal/mol higher than ext-CAS+1+2+Q value, with the perturbative estimate of triple excitations decreasing the barrier height by over 2.2 kcal/mol. In fact, the effect of the perturbative triples is over twice as large as in the F + H_2 reaction and emphasizes the relatively greater demands placed on the HF-based methods for this reaction. This is undoubtedly due to the more central location of the saddle point.

The calculated saddle point geometries shown in Table 2 generally exhibit less variation in the calculated O−H distances as a function of theoretical method and basis set in comparison to the H−F distance of F + H_2. On the other hand, since the H−H distance is longer in O + H_2 than in F + H_2, the calculated r_e(HH) values show relatively larger variations in regard to the correlation method and basis set used. In particular, the MP*n* values for r_e(HH) are much smaller than the CAS+1+2 results, and the triples correction to R-UCCSD leads to a substantial shortening of the H-H distance; see Figure 6. There is good agreement between the R-UCCSD(T) and ext-CAS+1+2 values, as was also the case in the F + H_2 reaction. In the case

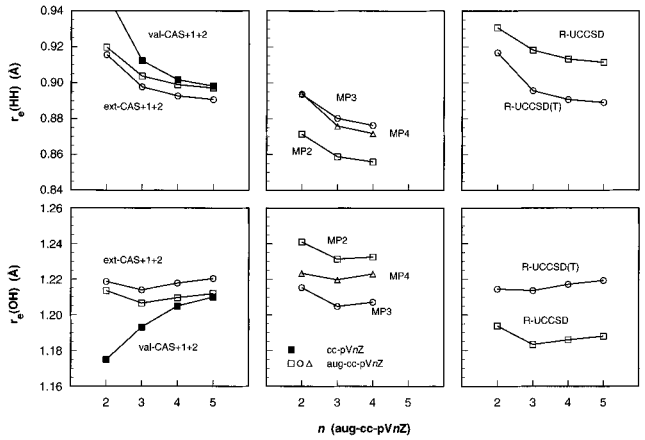

Figure 6. Calculated saddle point geometries, r_e(HH) and r_e(OH), for the O + H_2 abstraction reaction (in Å). Solid symbols denote the standard basis sets, open symbols the augmented basis sets.

of O+H_2, however, there is much less difference between the CAS+1+2 and CAS+1+2+Q geometries.

Results obtained using the different variants of open-shell CCSD(T) for the O+H_2 reaction are also shown in Table 5. As in F + H_2, the calculated R-UCCSD(T) reaction energy defect is midway between the values obtained with RCCSD(T) and U-UCCSD(T) and differs from these methods by just ~0.05 kcal/mol. At the saddle point, the RCCSD(T) method yields a barrier height nearly 0.6 kcal/mol higher than either of the spin unrestricted methods. In addition, the geometry of the saddle point calculated with this method differs significantly from that of R-UCCSD(T); the fitting errors were substantially larger as well.

The effects of correlating the 1s-like core electrons of oxygen are shown in Table 5 and yield almost identical core contributions as obtained for the F + H_2 reaction. The effect of core correlation on the barrier height is calculated to be just −0.03 kcal/mol, despite the more central location of the barrier to reaction. However, the core contribution to the bond dissociation energy of the OH radical is +0.14 kcal/mol, which decreases the reaction energy defect by this amount. When this contribution is added to ΔE_{rxn} from the R-UCCSD(T) calculations with the aug-cc-pV5Z basis set, a value of 2.55 kcal/mol is obtained, resulting in somewhat worse agreement with experiment.

The previously published MRCI calculations of Walch[26] predicted a reaction energy defect of 1.7 kcal/mol, a barrier height of 15.1 kcal/mol, and (with a smaller basis set) a saddle point geometry of r_e(HF) = 1.224 Å and r_e(HH) = 0.894 Å. Earlier MRCI calculations by Wright et al.[22] yielded a barrier height of 12.8 kcal/mol by using a basis set augmented by bond functions. More recent, unpublished calculations by Walch[27] with a partially augmented cc-pVQZ set yield results similar to the present work: ΔE_{rxn} = 3.2 kcal/mol, ΔE_b = 13.6 kcal/mol, and r_e(OH) = 1.214 Å and r_e(HH) = 0.899 Å.

H′ + HCl → H′Cl + H. Calculated results for the reactants and saddle point of the collinear H′ + HCl exchange reaction are shown in Table 3. For the reactants, there is again a relatively large effect on the D_e of HCl when the +Q correction is applied with the val-CAS+1+2 calculation. With the aug-cc-pV5Z basis set the resulting difference in D_e(HCl) is 1.43 kcal/mol. For the +Q method, the calculated value differs from experiment by just −0.19 kcal/mol. As also observed previously for the other reactions of this study, expanding the active space significantly increases (+0.75 kcal/mol) the CAS+1+2 value for D_e, while the +Q addition results in only a minor correction (−0.13 kcal/mol).

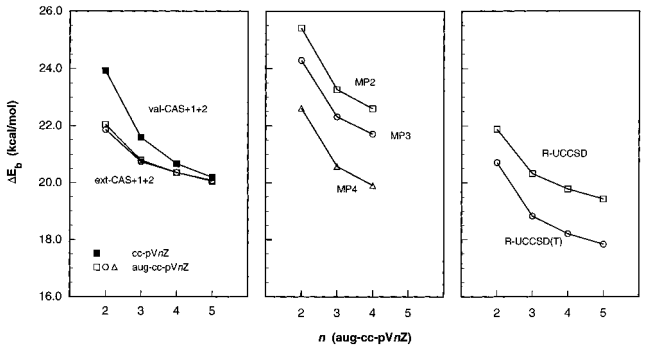

Figure 7. Calculated barrier heights, ΔE_b, for the H′ + HCl exchange reaction (in kcal/mol). Solid symbols denote the standard basis sets, open symbols the augmented basis sets.

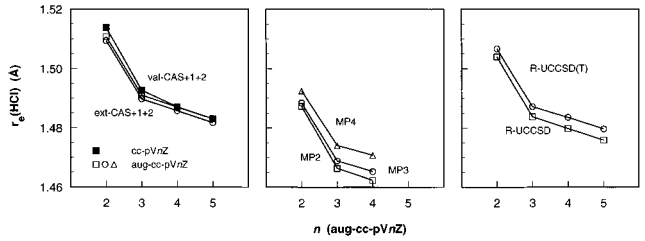

Figure 8. Calculated saddle point geometries, r_e(HCl), for the H′+ HCl exchange reaction (in Å). Solid symbols denote the standard basis sets, open symbols the augmented basis sets.

The ext-CAS active space for the H + HCl system corresponds to adding orbitals of π_x and π_y symmetry that are essentially of 3d character, whereas in the previous reactions they were of 3p character. Additional calculations were also completed where another set of orbitals of π_x and π_y symmetry that were essentially of 4p character were included in the reference function. These results, which were carried out with the aug-cc-pVQZ basis set, are also shown in Table 3 denoted by ext′-CAS+1+2. The larger active space yields a slightly longer bond length relative to ext-CAS+1+2, and the values for D_e are also increased by 0.28 and 0.12 kcal/mol for CAS+1+2 and CAS+1+2+Q, respectively.

For the HF-based methods, the R-UCCSD(T) results are again in excellent agreement with the ext-CAS+1+2+Q results for both the r_e and D_e of HCl. In this case, MP4 also appears to perform well for the reactants, leading to nearly identical values for these quantities, although D_e is slightly higher than that calculated with the R-UCCSD(T) method (and experiment). MP2 and MP3 yield bond energies that differ by just 0.3−0.9 kcal/mol from the MP4 results.

For the collinear, symmetric saddle point, smooth convergence of the calculated geometries and barrier heights is observed for each correlation method as a function of correlation consistent basis set; see Figures 7 and 8. While the effect of additional diffuse functions on ΔE_b is not as pronounced as in the abstraction reactions, it still leads to a lowering of the barrier by 0.8 kcal/mol even at the triple-zeta level. The effect, however, continues to decrease strongly as basis sets of quadruple- or quintuple-zeta quality are employed. This is reflected as well by the calculated HCl dissociation energies shown in Table 3.

In computing the barrier height with the CAS+1+2 methods, extending the active space from val-CAS to ext-CAS has essentially no effect at the CAS+1+2 level (20.06 vs 20.08 kcal/mol) and decreases the +Q value by just 0.18 kcal/mol, from 18.45 to 18.27 kcal/mol. Further expansion of the active space (ext → ext′) has a much stronger effect; the ext-CAS+1+2 and ext-CAS+1+2+Q barrier heights are decreased by 0.87

TABLE 7: Summary of Best Computed Results for Reaction Energy Defects (kcal/mol), Classical Barrier Heights (kcal/mol), and Transition State Geometries (Å) for the F + H_2, O + H_2, and H′ + HCl Reactions

				TS geometry	
reaction	method	ΔE_{rxn}	ΔE_b	r_e(HH)	r_e(HX)
F+H_2 → HF + H	ext-CAS+1+2+Q/aug-cc-pV5Z	−31.86	1.94	0.761	1.573
	estimated CBS	−32.17	1.88		
	+core−valence corr	−32.3	1.9		
	noncollinear[a]		1.5	0.770	1.549
O+H_2 → OH + H	ext-CAS+1+2+Q/aug-cc-pV5Z	2.70	13.27	0.894	1.215
	estimated CBS	2.44	13.15		
	+core−valence corr	2.3	13.1		
H′+HCl → H′Cl + H	ext-CAS+1+2+Q/aug-cc-pV5Z		18.27		1.481
	estimated CBS		18.19		
	ext → ext′ reference		17.98		
	+core−valence corr		18.0		

[a] The transition state geometry was obtained by applying the results from the noncollinear R-UCCSD(T) calculations (θ = 117.6°) to the CAS+1+2+Q collinear geometry.

and 0.21 kcal/mol, respectively. As shown in Table 3, however, the saddle point geometry is only marginally affected by expansion of the reference space.

The barrier heights calculated at the R-UCCSD(T) level are slightly lower than those obtained at either the ext-CAS+1+2+Q or ext′-CAS+1+2+Q levels, e.g., 18.21 vs 18.59 or 18.38 kcal/mol (aug-cc-pVQZ), respectively, with somewhat shorter bond lengths at the saddle point, e.g., 1.4836 Å vs 1.4847 or 1.4850 Å (aug-cc-pVQZ). Including the perturbative correction for triple excitations lowers the coupled cluster barrier height by 1.6 kcal/mol.

Even though the MP*n* methods yielded reasonable values for the dissociation energy of HCl, the resulting barrier heights are too high by several kcal/mol. Compared to the R-UCCSD(T) value with the aug-cc-pVQZ basis set, MP2 is higher by 4.4 kcal/mol, MP3 is higher by 3.5 kcal/mol, and even MP4 is too high by 1.7 kcal/mol. The saddle point bond lengths calculated by MP*n* are also substantially shorter than those obtained with the R-UCCSD(T) method.

In comparing the different variants of open shell CCSD(T) for the saddle point (Table 5), the RCCSD(T) method leads to a ΔE_b value that is larger than the R-UCCSD(T) value by about 0.4 kcal/mol with a slightly shorter bond length at the saddle point (by 0.002 Å). The effects of correlating the core electrons of Cl are shown in Table 6 and yield a core contribution of +0.19 kcal/mol for D_e(HCl) and just +0.04 kcal/mol for ΔE_b.

The SEC-corrected (scaled external correlation) MRCI surface of Schwenke et al. [28] and Allison et al. [29] yielded values of ΔE_b = 18.1 kcal/mol (the uncorrected value was 20.0 kca/mol) and r_e(HCl) = 1.479 Å, in good agreement with the present, more accurate calculations. These surfaces have been used in extensive dynamics calculations; see refs 64 and 65. Dobbs and Dixon[66] obtained an exchange barrier height of 20.2 kcal/mol for the H′ + HCl reaction using the CCSD(T) method. This is higher, however, than our best R-UCCSD(T) value (17.8 kcal/mol), predominately due to the neglect of diffuse functions in their basis set. The reader is directed to refs 29 and 66 for references to previous calculations and experiments on this reaction.

Conclusions

Using the correlation consistent basis sets, the reaction energy defects, barrier heights, and saddle point geometries for the abstraction reactions, F + H_2 and O + H_2, and the exchange reaction, H′ + HCl, have been investigated using several common methods for treating electron correlation (multireference configuration interaction, Møller−Pesset perturbation theory, and coupled cluster methods). Where experimental values are available, excellent agreement with experiment is obtained when either extended MRCI or CCSD(T) wave functions are employed. In each case the systematic convergence characteristics of the correlation consistent basis sets facilitated an unambiguous assessment of the complete basis set limit, and hence the *intrinsic accuracy*, of each correlation method. Table 7 summarizes the most accurate values of reaction energy defects and barrier heights obtained from the present study, and these results are discussed briefly below.

For the collinear F(^{2}P) + H_2 reaction, our best results for the barrier height and reaction energy defect were obtained with either the ext-CAS+1+2+Q or R-UCCSD(T) methods. After extrapolating to the complete basis set limit and including core−valence correlation effects , values of 1.88 and −32.3 kcal/mol were obtained for the collinear barrier height and exoergicity, respectively. The latter value differs from the experimental result by 0.2 kcal/mol. The collinear barrier height of 1.88 kcal/mol compares very well with the limit estimated by Stark and Werner[20] of 1.83 ± 0.05 kcal/mol. The R-UCCSD(T) method predicted the barrier height for the noncollinear saddle point to be 1.45 kcal/mol at the CBS limit. This result is in quantitative agreement with the previous MRCI calculations of Stark and Werner and the R-UCCSD(T) work of Scuseria.[61]

For the O(^{3}P) + H_2 reaction, our most accurate predicted values are obtained using ext-CAS+1+2+Q wave functions; however, the R-UCCSD(T) results differ only slightly. Including the core−valence correlation contributions and extrapolation to the CBS limit, a barrier height and reaction energy defect of 13.1 and 2.3 kcal/mol, respectively, are obtained. The latter value is smaller than the experimental result by nearly 0.6 kcal/mol due to an overestimation of the OH bond dissociation energy (and a slight underestimation of the H_2 bond energy). Our predicted barrier height can be compared to the externally contracted multireference CI (plus Davidson correction) result of Walch[26] of 12.7 kcal/mol. More recent calculations by Walch[27] using similar basis sets and correlation methods are in good agreement with our present values.

After accounting for the effects of core−valence correlation and extrapolating to the CBS limit, the barrier height for the H′ + HCl exchange reaction is predicted by ext-CAS+1+2+Q to be 18.2 kcal/mol. Further extension of the reference function in the MRCI, as indicated by the ext′-CAS+1+2 results, is expected to lower the barrier by about 0.2 kcal/mol, which yields a best estimate of 18.0 kcal/mol for the classical barrier. The R-UCCSD(T) calculation yields a very similar, if slightly smaller, value for the barrier height, 17.8 kcal/mol. The most accurate calculations to date are those of Schwenke *et al.*[28] who carried out MRCI (CAS+1+2) calculations with a large basis

set and then corrected the results with the SEC method. They obtained $\Delta E_b = 18.1$ kcal/mol (the uncorrected value was 20.0 kcal/mol) with $r_e(HCl) = 1.479$ Å. Their corrected result is in excellent agreement with our current value, where much more extensive correlation and basis set expansions were used. Recently, a new global $Cl+H_2$ surface has been calculated by Berning and Werner[67] using icMRCI wave functions with a aug-cc-pV5Z quality basis set. Their global fit yields an exchange barrier of 17.8 kcal/mol, which is in excellent agreement with the present work.

A few general observations can be drawn from the studies reported herein:

1. The ext-CAS+1+2+Q and R-UCCSD(T) methods provide essentially quantitative accuracy for the computed reaction energy defects, with typical errors of a few tenths of a kcal/mol when core−valence correlation effects are included.

2. The ext-CAS+1+2+Q and R-UCCSD(T) methods appear to provide high accuracy for the calculated barrier heights, although direct comparisons with experiment are not possible. The val-CAS+1+2 method yields barriers that are too large by as much as 2 kcal/mol.

3. The RCCSD(T) method yields barrier that are several tenths of a kcal/mol larger than obtained with the R-UCCSD(T) method, with corresponding differences in the saddle point geometries. The potential energy surfaces near the saddle points obtained from RCCSD(T) calculations were also less smooth (as evidenced by the polynomial fits) than those obtained from R-UCCSD(T) calculations, especially for $O + H_2$.

4. For the reactions considered here there is little difference between the results obtained from R-UCCSD(T) and U-UCCSD(T) calculations.

5. Perturbation theory methods through MP4 yield reaction energy defects and barrier heights that are in error by several kcal/mol. These methods are, therefore, not suitable for quantitative work. Spin projection may substantial improve the accuracy of the perturbation theory calculations (see Schlegel and Sosa[59]).

6. The additional diffuse functions in the aug-cc-pV*n*Z sets dramatically decrease the calculated barrier heights for the smaller basis sets, substantially improving the convergence of the basis set expansion.

Acknowledgment. This work was supported by the Division of Chemical Sciences in the Office of Basic Energy Sciences of the U.S. Department of Energy at Pacific Northwest National Laboratory, a multiprogram national laboratory operated by Battelle Memorial Institute, under Contract No. DE-AC06-76RLO 1830. K.A.P. also acknowledges the support of the Associated Western Universities, Inc., Northwest Division, under Grant No. DE-FG06-89ER-75522 with the U.S. Department of Energy. Computational resources for this work were provided by the Chemical Sciences Division, Office of Energy Research, and by the Mathematical, Information, and Computational Sciences Division, Office of Energy Research, at the National Energy Research Supercomputing Center (Livermore, California).

References and Notes

(1) Almlöf, J.; Taylor, P. R. *J. Chem. Phys.* **1987**, *86*, 4070.
(2) Widmark, P. O.; Malmqvist, P. Å.; Roos, B. O. *Theor. Chim. Acta* **1990**, *77*, 291.
(3) Widmark, P. O.; Persson, B. J.; Roos, B. O. *Theor. Chim. Acta* **1991**, *79*, 419.
(4) Dunning, T. H., Jr. *J. Chem. Phys.* **1989**, *90*, 1007.
(5) Kendall, R. A.; Dunning, T. H., Jr.; Harrison, R. J. *J. Chem. Phys.* **1992**, *96*, 6796.
(6) Woon, D. E.; Dunning, T. H., Jr. *J. Chem. Phys.* **1993**, *98*, 1358.
(7) Woon, D. E.; Dunning, T. H., Jr. *J. Chem. Phys.* **1994**, *100*, 2975.
(8) Woon, D. E.; Dunning, T. H., Jr. *J. Chem. Phys.* **1995**, *103*, 4572.
(9) Wilson, A. K.; van Mourik, T.; Dunning, T. H., Jr. *J. Mol. Struct. (THEOCHEM)* **1996**, *388*, 339.
(10) Woon, D. E.; Dunning, T. H., Jr. *J. Chem. Phys.* **1993**, *99*, 1914.
(11) Peterson, K. A.; Kendall, R. A.; Dunning, T. H., Jr. *J. Chem. Phys.* **1993**, *99*, 1930.
(12) Peterson, K. A.; Kendall, R. A.; Dunning, T. H., Jr. *J. Chem. Phys.* **1993**, *99*, 9790.
(13) Woon, D. E.; Dunning, T. H., Jr. *J. Chem. Phys.* **1994**, *101*, 8877.
(14) Peterson, K. A.; Dunning, T. H., Jr. *J. Phys. Chem.* **1995**, *99*, 3898.
(15) Peterson, K. A. *J. Chem. Phys.* **1995**, *102*, 262.
(16) Woon, D. E. *J. Chem. Phys.* **1994**, *100*, 2838.
(17) Peterson, K. A.; Dunning, T. H., Jr. *J. Chem. Phys.* **1995**, *102*, 2032.
(18) Peterson, K. A.; Woon, D. E.; Dunning, T. H., Jr. *J. Chem. Phys.* **1994**, *100*, 7410.
(19) Peterson, K. A.; Dunning, T. H., Jr. *J. Chem. Phys.* **1997**, *106*, 4119.
(20) Stark, K.; Werner, H.-J. *J. Chem. Phys.* **1996**, *104*, 6515.
(21) Manolopoulos, D. E.; Stark, K.; Werner, H.-J.; Arnold, D. W.; Bradforth, S. E.; Neumark, D. M. *Science* **1993**, *262*, 1852.
(22) Wright, J. S.; Donaldson, D. J.; Williams, R. J. *J. Chem. Phys.* **1984**, *81*, 397.
(23) Schaefer, H. F. I. *J. Phys. Chem.* **1985**, *89*, 5336.
(24) Walch, S. P.; Wagner, A. F.; Dunning, T. H., Jr.; Schatz, G. C. *J. Chem. Phys.* **1980**, *72*, 2894.
(25) Walch, S. P.; Dunning, T. H., Jr.; Raffenetti, R. C.; Bobrowicz, F. W. *J. Chem. Phys.* **1980**, *72*, 406.
(26) Walch, S. P. *J. Chem. Phys.* **1987**, *86*, 5670.
(27) Walch, S. P., private communication.
(28) Schwenke, D. W.; Tucker, S. C.; Steckler, R.; Brown, F. B.; Lynch, G. C.; Truhlar, D. G. *J. Chem. Phys.* **1989**, *90*, 3110.
(29) Allison, T. C.; Lynch, G. C.; Truhlar, D. G.; Gordon, M. S. *J. Phys. Chem.* **1996**, *100*, 13575.
(30) Feller, D. *J. Chem. Phys.* **1992**, *96*, 6104.
(31) Woon, D. E. *Chem. Phys. Lett.* **1993**, *204*, 29.
(32) Woon, D. E.; Dunning, T. H., Jr.; Peterson, K. A. *J. Chem. Phys.* **1996**, *104*, 5883.
(33) Del Bene, J. E. *J. Phys. Chem.* **1993**, *97*, 107.
(34) Peterson, K. A.; Dunning, T. H., Jr. *J. Mol. Struct. (THEOCHEM)*, in press.
(35) Peterson, K. A.; Dunning, T. H., Jr., manuscript in preparation.
(36) Purvis, G. D.; Bartlett, R. J. *J. Chem. Phys.* **1982**, *76*, 1910.
(37) Ragavachari, K.; Trucks, G. W.; Pople, J. A.; Head-Gordon, M. *Chem. Phys. Lett.* **1989**, *157*, 479.
(38) Hampel, C.; Peterson, K. A.; Werner, H.-J. *Chem. Phys. Lett.* **1992**, *190*, 1.
(39) Deegan, M. J. O.; Knowles, P. J. *Chem. Phys. Lett.* **1994**, *227*, 321.
(40) Møller, C.; Plesset, M. S. *Phys. Rev.* **1934**, *46*, 618.
(41) Knowles, P. J.; Hampel, C.; Werner, H.-J. *J. Chem. Phys.* **1994**, *99*, 5219.
(42) Scuseria, G. E. *Chem. Phys. Lett.* **1991**, *176*, 27.
(43) Rittby, M.; Bartlett, R. J. *J. Phys. Chem.* **1988**, *92*, 3033.
(44) Werner, H.-J.; Knowles, P. J. *J. Chem. Phys.* **1988**, *89*, 5803.
(45) Knowles, P. J.; Werner, H.-J. *Chem. Phys. Lett.* **1988**, *145*, 514.
(46) Langhoff, S. R.; Davidson, E. R. *Int. J. Quantum Chem.* **1974**, *8*, 61.
(47) Blomberg, M. R. A.; Siegbahn, P. E. M. *J. Chem. Phys.* **1983**, *78*, 5682.
(48) Simons, J. *J. Phys. Chem.* **1989**, *93*, 626.
(49) Peterson, K. A., Ph.D. Thesis, University of Wisconsin, 1990.
(50) Senekowitsch, J., Ph.D. Thesis, Universität Frankfurt, Frankfurt, Germany, 1988.
(51) MOLPRO is a package of *ab initio* programs written by H.-J. Werner and P. J. Knowles with contributions from J. Almlöf, R. D. Amos, M. J. O. Deegan, S. T. Elbert, C. Hampel, W. Meyer, K. A. Peterson, R. M. Pitzer, A. J. Stone, P. R. Taylor, and R. Lindh.
(52) ACES II is a computational chemistry package especially designed for CC and MBPT energy and gradient calculations. Elements of this package are as follows: the SCF, integral transformation, correlation energy, and gradient programs written by J. F. Stanton, J. Gauss, J. D. Watts, W. J. Lauderdale, and R. J. Bartlett; the VMOL integral and VPROPS property integral programs written by P. R. Taylor and J. Almlöf; a modified version of the integral derivative program ABACUS written by T. Helgaker, H. J. Jensen, P. Jørgensen, J. Olsen, and P. R. Taylor; and the geometry optimization and vibrational analysis package written by J. F. Stanton and D. E. Bernholdt.
(53) Gaussian 94, Revision D.1; Frisch, M. J.; Trucks, G. W.; Schlegel, H. B.; Gill, P. M. W.; Johnson, B. G.; Robb, M. A.; Cheeseman, J. R.; Keith, T.; Petersson, G. A.; Montgomery, J. A.; Raghavachari, K.; Al-Laham, M. A.; Zakrzewski, V. G.; Ortiz, J. V.; Foresman, J. B.; Cioslowski, J.; Stefanov, B. B.; Nanayakkara, A.; Challacombe, M.; Peng, C. Y.; Ayala, P. Y.; Chen, W.; Wong, M. W.; Andres, J. L.; Replogle, E.

S.; Gomperts, R.; Martin, R. L.; Fox, D. J.; Binkley, J. S.; Defrees, D. J.; Baker, J.; Stewart, J. P.; Head-Gordon, M.; Gonzalez, C.; Pople, J. A. Gaussian, Inc., Pittsburgh, PA, 1995.

(54) Martin, J. M. L.; Taylor, P. R. *Chem. Phys. Lett.* **1994**, *225*, 473.

(55) Moore, C. E. *Atomic Energy Levels*; NSRDS-NBS 35, Office of Standard Reference Data, National Bureau of Standards: Washington, D.C., 1971.

(56) Huber, K. P.; Herzberg, G. *Molecular Spectra and Molecular Structure IV. Constants of Diatomic Molecules*; Van Nostrand: Princeton, NJ, 1979.

(57) Bauschlicher, C. W., Jr.; Langhoff, S. R.; Lee, T. J.; Taylor, P. R. *J. Chem. Phys.* **1989**, *90*, 4296.

(58) Knowles, P. J.; Stark, K.; Werner, H.-J. *Chem. Phys. Lett.* **1991**, *185*, 555.

(59) Schlegel, H. B.; Sosa, C. *Chem. Phys. Lett.* **1988**, *145*, 329.

(60) Wright, J. S.; Kolbuszewski, M.; Wyatt, R. E. *J. Chem. Phys.* **1992**, *97*, 8296.

(61) Scuseria, G. E. *J. Chem. Phys.* **1991**, *95*, 7426.

(62) Kraka, E.; Gauss, J.; Cremer, D. *J. Chem. Phys.* **1993**, *99*, 5306.

(63) Frisch, M. J.; Liu, B.; Binkley, J. S.; Schaefer, H. F.; Miller, W. H. *Chem. Phys. Lett.* **1985**, *114*, 1.

(64) Mielke, S. L.; Allison, T. C.; Truhlar, D. G.; Schwenke, D. W. *J. Phys. Chem.* **1996**, *100*, 13588.

(65) Alagia, M.; Balucani; Cartechini, L.; Casavecchia, P.; van Kleef, E. H.; Volpi, G. G.; Aoiz, F. J.; Bänares, L.; Schwenke, D. W.; Allison, T. C.; Mielke, S. L.; Truhlar, D. G. *Science* **1996**, *273*, 1519.

(66) Dobbs, K. D.; Dixon, D. A. *J. Phys. Chem.* **1993**, *97*, 2085.

(67) Werner, H.-J., private communication.